

Block Copolymer of *trans*-Polyisoprene and Urethane Segment: Crystallization Behavior and Morphology

Xiaohui Sun, Xiuyuan Ni

Department of Macromolecular Science, Fudan University, The Key Laboratory of Molecular Engineering of Polymers, Ministry of Education, Shanghai 200433, People's Republic of China

Received 30 April 2003; accepted 31 May 2004

DOI 10.1002/app.21016

Published online 22 October 2004 in Wiley InterScience (www.interscience.wiley.com).

ABSTRACT: A new type of urethane segmented copolymer was prepared from hydroxyl-terminated *trans*-polyisoprene (HTPI) and toluene diisocyanate (TDI). The structures of the copolymer were characterized by FTIR and GPC. Crystalline properties of *trans*-polyisoprene (TPI) segments were investigated using WAXD and DSC techniques. The crystals of TPI segments are inclined to exist in low-melting form (LM). The melting temperature of TPI shifts to a lower temperature as the urethane segment was introduced. DMA studies show that, when TPI crystals were at the melting state, the storage modulus of the copolymer depended on

the content of urethane segment. The hard segment here serves as physical crosslinkage. Nonisothermal crystallization kinetics of TPI segment was studied on the basis of the Ozawa equation. It was found that the hard segment suppresses the crystallization of the TPI segment. Morphology of two-phase separation was observed in the copolymer by SEM. © 2004 Wiley Periodicals, Inc. *J Appl Polym Sci* 94: 2286–2294, 2004

Key words: block copolymers; *trans*-polyisoprene; crystallization; morphology; shape memory

INTRODUCTION

Polyurethanes are segmented copolymers consisting of soft segment domains derived from a polyol monomer and hard segment domains derived from a diisocyanate and a chain extender.¹ The hard-segment domains, dispersing in the soft matrix, act as physical junction points. In conventional polyurethanes the soft segment is a polyether or polyester polyol. A number of investigations has focused on novel polyurethanes based on nonpolar macromolecular polyols such as polyisobutylene, polybutadiene, and *cis*-polyisoprene polyols.^{2–4} In the nonpolar polyol-based polyurethanes there is not a hydrogen bonding between the soft segment and the hard segment. The hydrogen bonding but also other interactions are just confined to the hard-segment domains. As a result, the segmented copolymers usually exhibit a more complete microphase separation relative to those based on the polar polyols, along with a high tensile, superior water-resistant properties and a high modulus.³ The polymers, in addition, can serve as model compounds of interests for theoretical study of structure–property relations,² because the influences of thermodynamic interactions are considered negligible.

In this paper we prepare segmented copolymers from hydroxyl-terminated *trans*-polyisoprene (HT-

TPI), toluene diisocyanate (TDI), and 1,4-butanediol as the chain extender. *trans*-1,4-Polyisoprene (TPI) has the same chemical “building block” as natural rubber (*cis*-1,4-polyisoprene) but special configuration. The polymer is easy to crystallize owing to its regular structure. TPI is of polymorphism and the crystals exist in two forms, i.e., high melting form (HMF) and low melting form (LMF).^{5–8} Because of the crystalline nature, TPI displays plastic behaviors quite different from the flexibility of natural rubber. TPI is not found today in applications other than antiques and fabrication of golf balls. The TPI-segmented copolymer synthesized in this paper is a new material based on TPI. The monomer HTPI was prepared according to the procedures of the photochemical degradation developed by Ravindran et al.⁹ Our primary experiments implied that TPI segments can crystallize depending on the content of urethane segment. Generally, in semicrystalline copolymers, the crystalline block plays an important role in the microphase separation and formation of high-order structures.^{10–12} The objectives of the present study were to investigate the crystallization behaviors of TPI segments and to understand the effects of the hard segment incorporated on the crystallization of TPI segments.

According to the molecular mechanism of shape memory effects of polymers,^{13,14} TPI segmented copolymer can exhibit shape memory effects responsive to the thermal stimuli. For a shape memory polyurethane, the crystalline soft segment serves as

Correspondence to: X. Ni (xyeni@fudan.edu.cn).

a molecular switch and enables the fixation of the temporary shape. The hard segment serves as the physical crosslinkage and is responsible for the permanent shape. If the polymer in the temporary shape is heated up, the permanent shape can be recovered. The transition temperature of the polymer is the melting temperature of the soft segment. It is believed that the crystalline properties of TPI segments in the copolymer affect the shape memory temperature and the ability of the copolymer to memorize its permanent shape. Knowledge of the crystallization behaviors of TPI segments allows a proper designing of shape memory materials from the TPI-urethane segmented copolymer.

EXPERIMENTAL

Materials

HTTPI with $\bar{M}_n = 3.2 \times 10^4$, $\bar{M}_w/\bar{M}_n = 1.8$ was used. The molecular weight is measured using gel permeation chromatography (GPC). The hydroxyl value was estimated according to the method of ASTM D1957–86. Toluene diisocyanate (a 80/20 mixture of 2,4 and 2,6 isomers) was supplied by Medicine and Chemicals Co. of China. 1,4-Butanediol was used as received. Dibutyltin dilaurate (DBTDL) was used as a catalyst for the reaction of hydroxyl groups with isocyanates. Toluene was of reagent grade, distilled before use.

Synthesis of TPI-urethane copolymers

TPI-urethane copolymers were prepared by a two-shot process of polyurethane synthesis. HTTPI was dissolved in 30 mL toluene in a round-bottomed, four-necked flask equipped with a mechanical stirrer, nitrogen inlet, and a reflux condenser. Two to three drops of DBTDL catalyst was added into the solution. After the solution was stirred for 30 min, a desired stoichiometric amount of TDI was added dropwise into the solution over a period of 90 min and the reaction was continued for 60 min to ensure endcapping of HTTPI. A required quantity of 1,4-butanediol was then added over a period of 45 min. The reaction was continued for 3 h at 80°C.

Solution crystallization

The polymer product obtained was dissolved in hexane at a dilute concentration of 0.2% wt/vol. The polymer solution was placed at -20°C for 24 h for crystallization. The crystalline samples, participated from the solution, were filtered and dried under vacuum at room temperature before tests.

Gel permeation chromatography

The molecular weights of HTTPI and the synthetic copolymers were measured by GPC (HP Aligent 1100) and calibrated by standard polystyrene. The solvent was THF and the fluent rate was 1.0 mL/min.

Spectroscopic analysis

FTIR spectroscopy was recorded on Magna-IRTM550 (Nicolet). ¹H-NMR spectra were recorded on a DMX 500 NMR spectrometer at 500 Hz using deuterated chloroform (CDCl₃) as solvent and tetramethylsilane (TMS) as an internal standard.

Differential scanning calorimetry

DSC curves were recorded on a Perkin–Elmer Pyris 1 DSC instrument. The sample was scanned from 20 to 80°C at a heating rate of 10°C/min. During the tests of the nonisothermal crystallization, each of the crystalline samples (about 4 mg) was heated to 140°C in nitrogen atmosphere and stayed at this temperature for 5 min to eliminate the thermal history. It was subsequently cooled to -10°C at cooling rates of 2.5, 5.0, 10, and 20°C/min, respectively. The fusion heat of the TPI crystals was taken as 140.82 J/g^{6,15} for calculations of the degree of crystallinity.

Wide angle X-ray diffraction (WAXD)

Wide angle X-ray diffractograms were recorded on a D/Max—III A diffractometer at 300 K. The scanning range was 5° to 50° at a rate of 4° θ /min. The wavelength of the beam was 1.5418 Å (CuK α line). The values of the crystallinity were calculated using the X-ray diffraction software by Tsing-hua University.

Scanning electron microscopy

To study the microphase structure of the copolymer and the crystalline morphology of the samples prepared from the solution crystallization, scanning electron microscopy (HITACHI S-520) at 20 KV was used. Fracture surfaces were prepared at the room temperature and coated with gold using a Eiko IB3 coater.

Dynamic mechanical analysis

The samples in film were prepared by casting the solution of the copolymer onto a PTFE plate and heating at 70°C for 24 h. Prior to the dynamic mechanical analysis, the samples were placed at room temperature for at least 2 weeks to ensure relaxation. DMA was carried out using a dynamic mechanical thermal analyzer (Netzsch DMA 242) at 10 Hz and at a heating rate of 5°C/min.

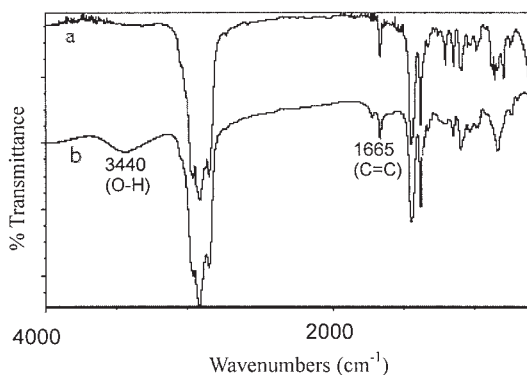


Figure 1 FTIR spectra of TPI (a) and HTTPI (b).

RESULTS AND DISCUSSION

Proofs of hydroxyl groups in HTTPI

The stretching vibration of hydroxyl groups at $3,442\text{ cm}^{-1}$ was clearly observed in the FTIR spectrum of HTTPI (Fig. 1), confirming hydroxyl groups in HTTPI. In the $^1\text{H-NMR}$ spectrum of HTTPI [Fig. 2(b)], the chemical shift of methyl proton is 1.59 ppm for *trans*-1,4 structure and 1.67 ppm for *cis*-1,4 structure, respectively.⁶ From the ratio of areas of the two peaks, the *trans*-1,4 content of HTTPI is estimated to be close to that of TPI [Fig. 2(a)]. As a consequence, the *trans*-configuration can be well retained in HTTPI regardless of the photochemical modification. Figure 2(c) shows the $^1\text{H-NMR}$ spectrum of HTTPI treated with deuterated water (D_2O). It is found that the exchange with D_2O causes the peak at 3.5 ppm of HTTPI to disappear. This allows identification of the peak as the protons of the hydroxyls, and thus provides extra evidence of hydroxyl groups in HTTPI in addition to the FTIR proof.

The functionality of HTTPI was measured to be close to that of hydroxyl-terminated natural rubber (HTNR) prepared through the photochemical degradation of natural rubber (NR).¹⁶ The functionality of the polymer was measured to be 1.84. It is considered that the reaction mechanism of TPI is the same as that of NR owing to the same method of photochemical degradation employed.

Structure of the segmented copolymer

Figure 3 shows the FTIR spectrum of the TPI-urethane copolymer synthesized. After HTTPI is reacted, the diagnostic absorption of OH groups ($3,440\text{ cm}^{-1}$) is found to disappear. A newly appeared peak at $3,313\text{ cm}^{-1}$ is the diagnostic absorption of N-H stretching. On the basis of the FTIR identifications for polybutadiene segmented polyurethanes,¹⁷⁻¹⁹ the peak at $1,720\text{ cm}^{-1}$ here is indicative of C=O stretching. The peaks at $1,535$ and

$1,230\text{ cm}^{-1}$ are assigned to NH bending and CN stretching in the copolymer. To ensure a complete convert of hydroxyls, the excess isocyanate was used in this study. The peak at $2,270\text{ cm}^{-1}$ is indicative of the unreacted isocyanate groups remaining in the copolymer.

Table I lists the molecular weights of the copolymer synthesized. The most interesting result to arise from Table I is that the copolymer is different in structures from the common polyurethanes prepared via the

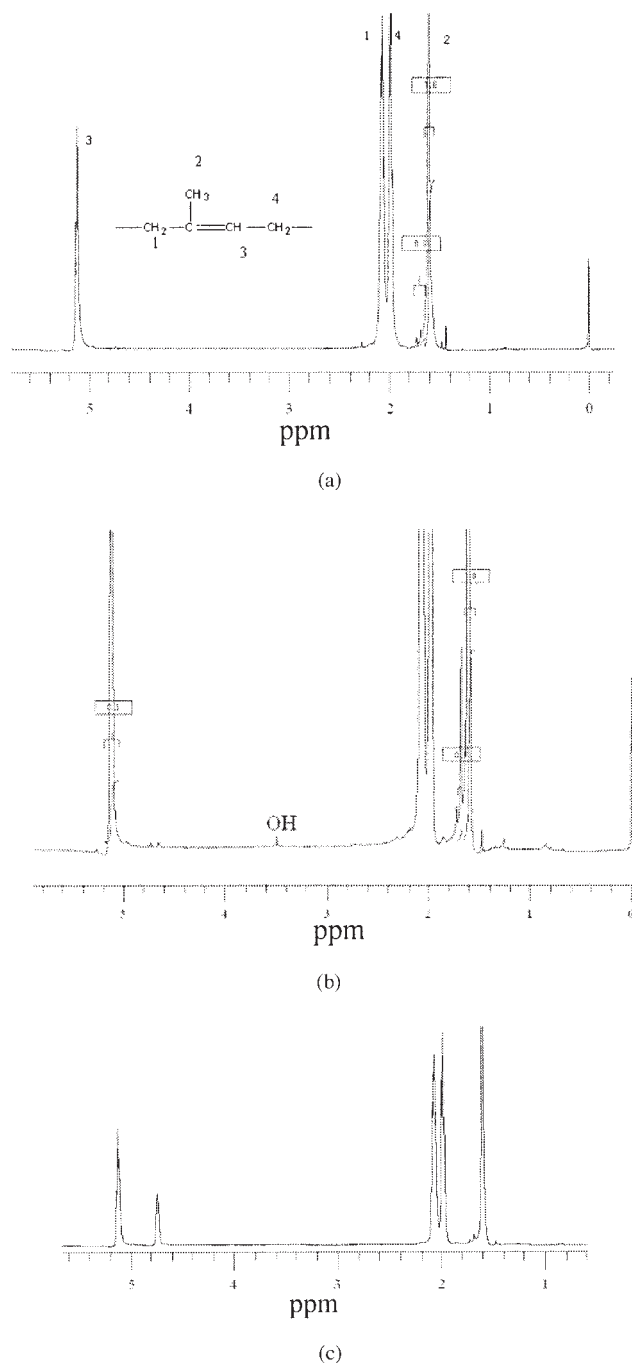


Figure 2 $^1\text{H-NMR}$ spectra of TPI (a), HTTPI (b), and the sample of HTTPI exchanged with D_2O (c).

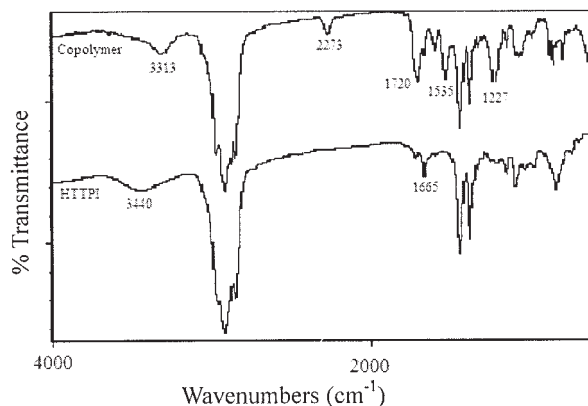


Figure 3 FTIR spectrum of the TPI-urethane copolymer.

two-shot process (Scheme 1). The data in the table shows that \bar{M}_n of the copolymer is higher than that of the starting HTTPI, confirming the successful incorporation of the urethane segment onto HTTPI chains. However, \bar{M}_n for most of the copolymers doesn't exceed the value as twice \bar{M}_n of the starting HTTPI. The result indicates that the copolymer may be two-block or triblock, different from the multiblock structure of the common polyurethanes. It is most likely that the chain of the copolymer consists of one TPI-segment end-capped with urethane segments. It is believed that in this case there has been the reaction of HTTPI with diisocyanate taking place in the same way as the usual two-shot process but special with chain-extension with 1,4-butanediol.

To be consistent with the terms of the common polyurethanes, the TPI segment in the copolymer is called the soft segment and the urethanes are the hard segment. The TPI-segmented copolymer is a new type of urethane copolymer based on nonpolar polyols. Apart from the structure, the copolymer is characterized as having no significant interaction between the soft segment and the hard segment.

Crystallization behaviors of TPI segments

In order that the crystalline properties of the TPI segment can be clearly revealed, solution-grown crystallization was employed. The urethane segment is insoluble in the solvent of hexane, whereas the TPI segment has certain solubility in the solvent. Their difference in solubility may lead to a complete two-phase separation in the solution, where each moiety manages to behave with its own properties during the crystallization. It is worthwhile to mention that many studies concerning solution crystallizations of polyolefins have found that the polymer crystals generated almost appear in single form.^{8,20} Although TPI usually crystallizes in two forms (HM and LM), the polymer is

ready to crystallize into the HM crystals during the solution crystallization at -20°C .²⁰ An interesting question arising is whether the urethane segment introduced affects the crystal forms of TPI.

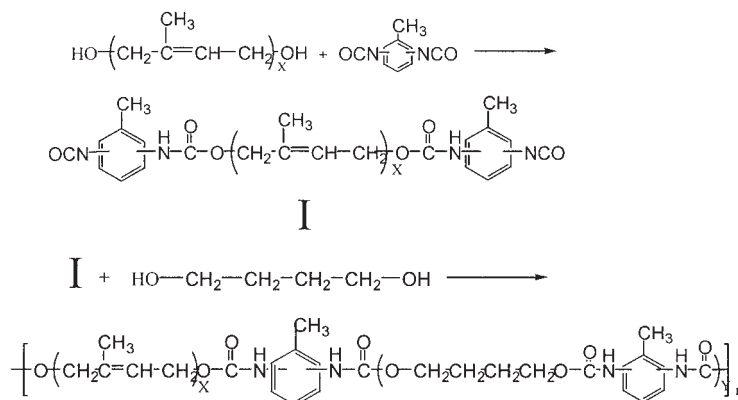
Figure 4 shows WAXD patterns of the copolymer samples obtained from the solution crystallization. The hard segment contents of the samples have been listed in Table I. The data dotted on the curves are the values of interplanar spacings (d) of the polymer crystals. All the interplanar spacings detected for the copolymer are consistent with that of the pure TPI.⁶ Any other crystalline signals exclusive of TPI crystals were not observed in the patterns, indicating the amorphous structure of the hard segment. Hopff and Susich²¹ have identified each of the interplanar spacings of TPI to the different crystal forms: the four interplanar spacings of 4.9, 4.6, 3.9, and 3.3 Å to HM crystals; the three interplanar spacings of 4.7, 3.9, and 2.9 to LM crystals. The information enables us to conclude that both HM crystals and LM crystals are produced simultaneously during the solution crystallization of the copolymer. It is important to find that the signals of LM crystals are intensified with the increase in urethane content. The result implies that the urethane segment inclines the TPI segment to crystallize into LM crystals.

Figure 5 shows DSC curves of the copolymer with different TPI contents at a fixed heating rate of $10^\circ\text{C}/\text{min}$. Both the endotherm peak of HM crystals and the peak of LM crystals are clearly observed. The melting temperature of each peak is found to shift toward lower temperature while the content of hard segment increases. The peak of LM crystals becomes stronger when the content of the hard segment increases. The result agrees with the conclusion drawn from the WAXD patterns. In Figure 5 there is a small peak appearing at 20°C along with the endotherm peaks of HM and LM crystals. A similar phenomenon was also observed by Edward and David²² and the forming mechanism remains unknown as yet.

Figure 6 shows the crystallinity of the soft segment plotted against the content of the hard segment. As observed in this figure, the crystallinity of TPI de-

TABLE I
 \bar{M}_n of the Copolymers and the Calculated Values of the Urethane Segment Content

\bar{M}_n of HTTPI ($\times 10^4$)	\bar{M}_n of Copolymer ($\times 10^4$)	Urethane segment content (%)	Samples in Figure 4
3.2	7.0	54.5	a
3.2	6.7	52.2	b
3.2	5.8	44.8	c
3.2	4.3	25.6	d
3.2	3.9	17.9	e
3.2	3.2	0	f



Scheme 1. Reaction pathway to urethane copolymer (two-shot process).

creases with the content of the hard segment increasing. There have been many studies that have elucidated comprehensively the crystalline properties of TPI;^{5-8,20,22} polymers of modified TPI were not involved, in contrast. Our studies find that TPI block in the copolymer is still capable of crystallizing but displays the crystallization behaviors distinguishing it from that of TPI. It appears that the modification to TPI would serve as an effective tool to obtain TPI based materials with a desired crystalline property.²³

Dynamic mechanical properties

The dynamic mechanical features of TPI-urethane copolymers can be seen in Figures 7 and 8 presenting the storage modulus E' and $\tan \delta$. The peak of $\tan \delta$ around 50°C is assigned to the melting point of TPI. The peak at -50°C is assigned to the glass transition of TPI segments. It is seen that the melting point of TPI inclines to shift to a lower temperature when the content of hard segment increases. This phenomenon is easily understood in consideration of the fact that LM

crystals of TPI are promoted in presence of the urethane segment (Fig. 5).

E' is a measure of material stiffness and can be used to provide information regarding polymer molecular weight and crosslink density. For shape memory materials, E' at the melting state is important to fabricate the temporary shape. Figure 8 shows that, at a fixed molecular weight of the soft segment, the modulus at the melting state increases with the content of the hard segment. A similar phenomenon has been detected by Kim et al.²⁴ for a shape memory polyurethane. It was considered that, in case the soft segment is melted, the modulus of the copolymer is devoted by the urethane segments acting as the physical crosslinkages.

For the shape memory polymers based on thermal stimuli, the copolymer consisting of a crystalline block is typically encountered. This is the case for the TPI-urethane copolymer synthesized in this paper. As mentioned earlier, the TPI segment takes the role of the switching molecule. The urethane segment acts as the physical crosslinkage. The transition temperature is determined by the melting temperature of the TPI

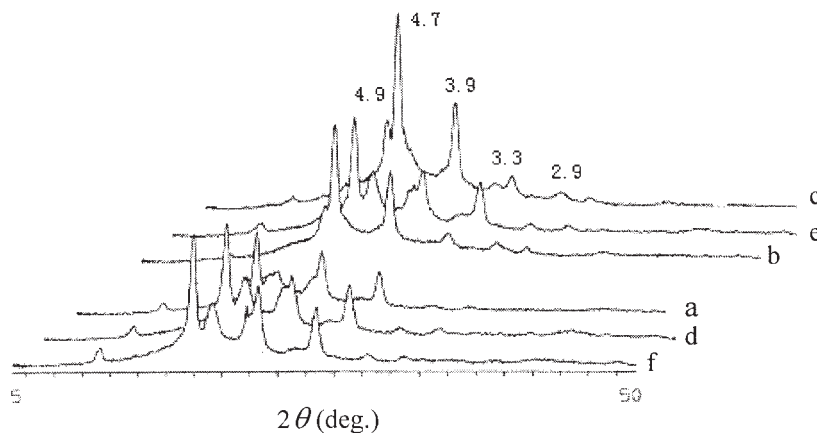


Figure 4 WAXD patterns of TPI-urethane copolymers. Urethane-segment contents of the samples are listed in Table I.

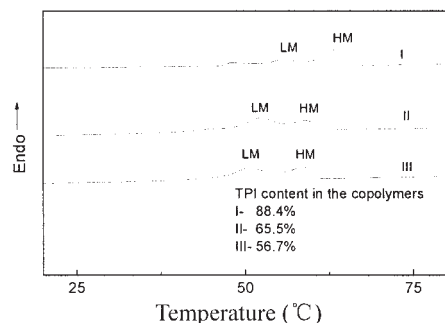


Figure 5 DSC curves of TPI-urethane copolymers at a heating rate of $10^{\circ}\text{C}/\text{min}$.

segment. The results of this study, regarding the interrelations of the hard segment content and the crystalline properties of TPI, are expected to play an important role in designing shape memory materials from the copolymer.

Crystallization kinetics of TPI segments

In view of the nonisothermal processing of shape memory materials, it is meaningful to assess the nonisothermal crystallization of the copolymer. Figure 9 shows the nonisothermal crystallization curves of the copolymers at different cooling rates. The curves of the pure TPI are shown in Figure 10. For each of the two polymers, the initial temperature of crystallization (T_0) shifts to a lower temperature when the cooling rate increases. The exotherm peak temperature (T_{max}) exhibits the same tendency, but T_{max} of TPI segments decreases more sharply relative to the pure TPI, as shown in Figure 11. The figure also shows that, at a fixed cooling rate, the urethane segments make T_{max} change in the direction of a lower temperature.

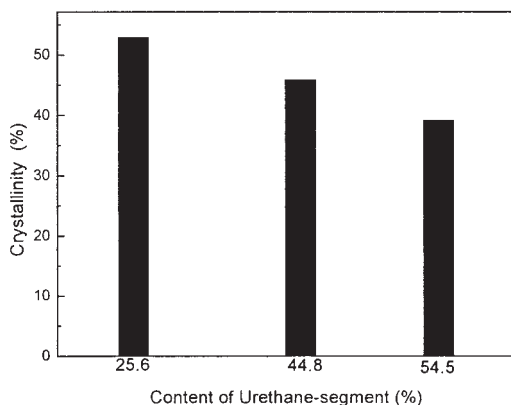


Figure 6 The degree of crystallinity of the copolymer versus the content of urethane segment.

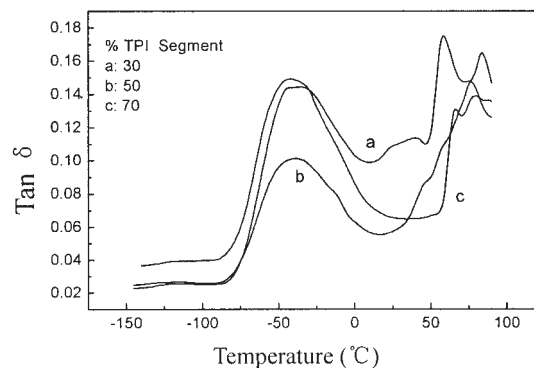


Figure 7 $\text{Tan } \delta$ of the film of the copolymer with TPI content: 30% (a); 50% (b); 70% (c).

Efforts are made to describe the kinetic of the nonisothermal crystallization on the basis of Ozawa²⁵ equation as follows:

$$\log[-\ln(1 - X_T)] = \log K(T) - n \log D \quad (1)$$

where X_T is the crystal conversion at a temperature T . D is the cooling rate. K is the cooling constant. n is the Avrami exponent. The Ozawa equation was developed from the Avrami equation of isothermal crystallizations and has been wide used to describe the processes of nonisothermal crystallizations of polyolefins.²⁵ From this equation, it follows that the slope of the plot, $\log[-\ln(1 - X_T)]$ versus $\log D$, represents the value of n and the intercept is a measure of the rate of nonisothermal crystallization.²⁶

Figure 12 shows Ozawa plots of the copolymer and the pure TPI. The plot of the copolymer is found to possess a lesser intercept and a lower slope relative to the pure TPI. It is apparent that the urethane segment suppresses the crystallization rate of the TPI segment

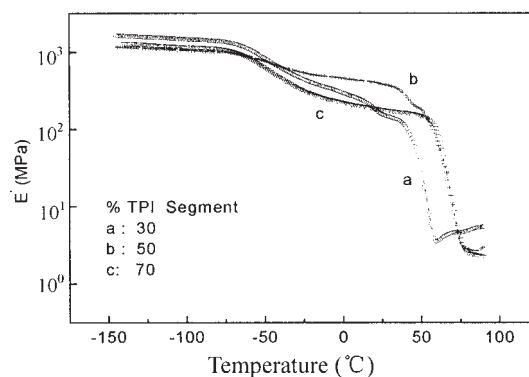


Figure 8 Storage modulus of the film of the copolymer with TPI content: 30% (a); 50% (b); 70% (c).

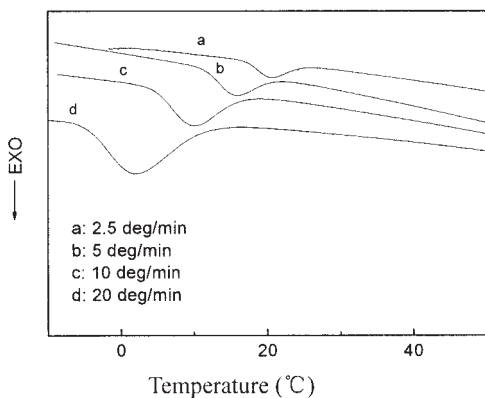


Figure 9 Thermograms of nonisothermal crystallization of TPI-urethane copolymer at various cooling rates.

and brings about a lower value of n . Since the Avrami exponent n is associated with dimensions of growth including space dimensions and time dimensions,²⁵ it is thus clear that the urethane segment may limit the growth of the crystals in space. In this case, the arrangement of TPI chains may also be influenced by the urethane segment so that the crystals in various forms can be produced.

Figure 13 shows the exotherm curves of the copolymers with different TPI contents at a fixed cooling rate of 10°C. When the urethane content increases, both T_{\max} and T_0 shift to lower temperatures, as shown in Figure 14. The value of $(T_0 - T_{\max})$ is a measure of the overall rate of crystallization.²⁷ The higher the value of $(T_0 - T_{\max})$, the lower the rate of the crystallization. Figure 15 shows that the value of $(T_0 - T_{\max})$ increases with the content of the hard segment. It indicates that the urethane segment suppresses the crystallization rate of the TPI segment. This result is in a good agreement with the conclusion drawn from the kinetic studies based on the Ozawa equation.

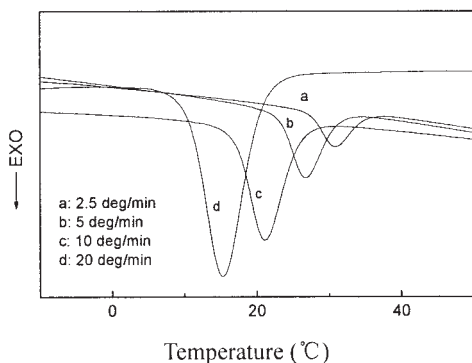


Figure 10 Thermograms of nonisothermal crystallization of TPI at various cooling rates.

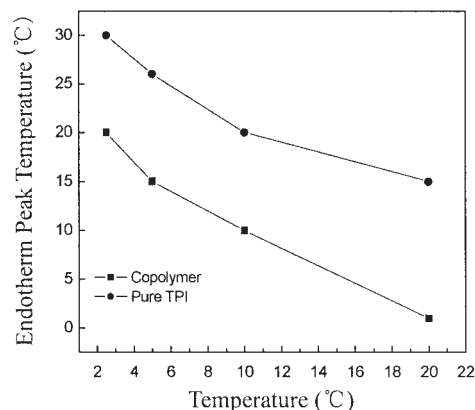


Figure 11 Demonstration of the shifts in the exotherm peak temperature as a function of the cooling rate.

Morphology of TPI-urethane copolymer

Figure 16 shows SEM photographs of the copolymer samples obtained from the solution crystallization. A well-defined microphase separation is observed. The domains of the urethane segments are well organized into spherical beads. Since there is hydrogen bonding among the urethane chains but no significant interaction between TPI and urethane segments, a self-assembly is expected to occur among the urethane segments. The formation of the spherical domains for the hard segments is considered to be a result from the strong self-assembly of the urethane chains. It has been mentioned earlier that any other crystal signals exclusive of TPI crystals were not observed in the WAXD patterns; the domains of the hard segment are therefore considered amorphous. From a point of view of the chain structure, the uneven disposition of the $-NCO$ group onto TDI molecules actually inhibits the chain alignment of the urethane from forming crystalline superstructures.

Apart from the beads of the urethane moiety, the morphology of the TPI moiety is clearly observed in

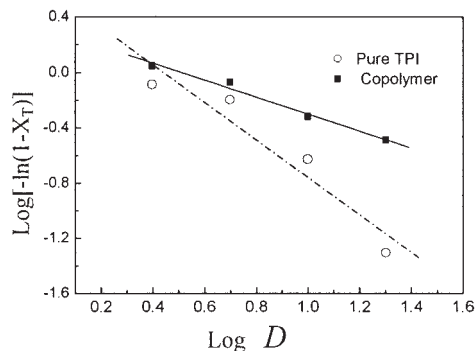


Figure 12 Plots of $\log[-\ln(1 - X_T)]$ against $\log D$ at the temperature of 0°C.

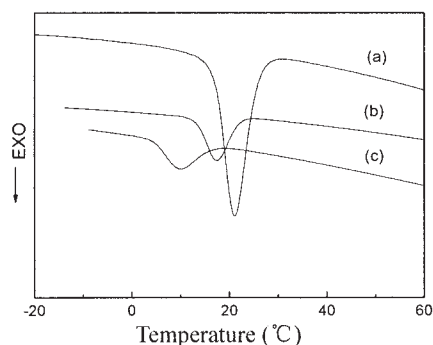


Figure 13 Thermograms of nonisothermal crystallization of the copolymer at the cooling rate of 10°C/min. TPI content: 100% (a); 97.4% (b); 54.0% (c).

the photographs. It is seen that the TPI segments can form the spherical-like regular congeries growing from lamellar crystals [Fig. 16(a)]. Because of the regular *trans*-conformation of TPI, the polymer inclines to arrange regularly, especially in a dilution solution.²⁰ It has been elucidated in this paper that the *trans*-configuration can be well retained in HTTPI regardless of the photochemical modification. So that TPI segments of the copolymer are able to rearrange in the dilution solution to form crystals.

It is observed that the boundary of the hard phase turns blurry at an enhanced soft-segment content, simultaneously the congeries of TPI segments are somewhat irregular [Fig. 16(b)]. It suggests that the morphology of the copolymer depends on its composition. Because of the poor interaction between the two segments, poor adhesion is reasonably expected to occur between the two phases. A copolymer with a complete phase separation usually exhibits high tensile modulus. The poor adhesion of the phase usually gives a relatively low elasticity. The TPI-segmented copolymer synthesized in this study is probably stiff and can find applications in surgery splint materials. The me-

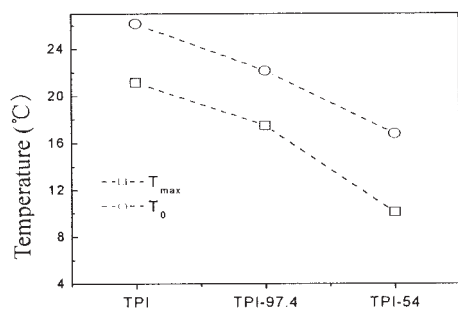


Figure 14 Demonstration of the shifts in T_{\max} and T_0 as a function of the TPI content.

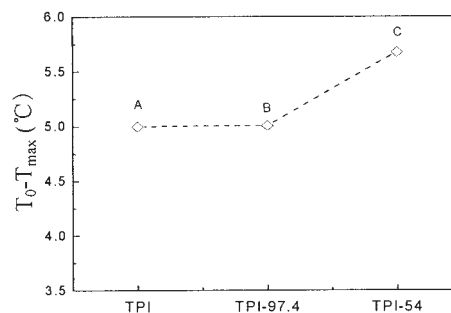


Figure 15 Demonstration of the value of $(T_0 - T_{\max})$ as a function of the TPI content.

chanical properties and shape memory effects of the copolymers will be described in another paper.

CONCLUSION

A novel type of urethane-segmented copolymer was synthesized. The TPI segments in the copolymer keep the crystallizability but its crystallinity decreases with an increase in the content of the hard segment. The presence of the hard segment makes the melting points of the TPI crystals shift to lower temperatures. The crystals of the TPI segment in the copolymer are ready to exist in LM form. The studies of nonisothermal crystallization show that the crystallization rate of TPI is suppressed by the hard segment. Because there is strong interaction among the urethane chains and no interaction exists between TPI and urethane segments, the two segments are incompatible. The microphase separation was clearly observed in the copolymer samples prepared from the solution-grown crystallization. The phase boundary is distinct. The copolymer synthesized in this study can have shape memory effects.

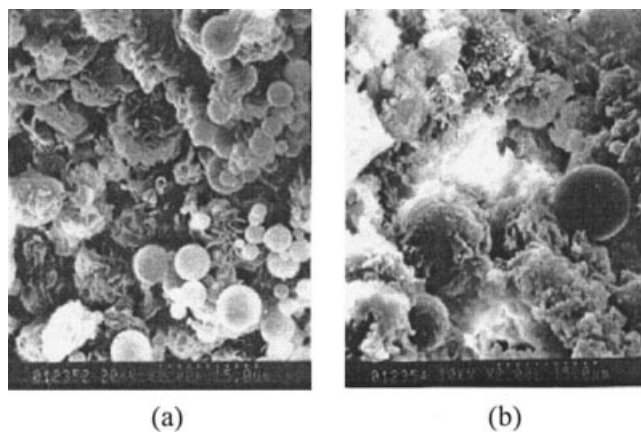


Figure 16 SEM photographs of the copolymers. Urethane content: 54.4% (a); 17.9% (b).

References

1. Bengston, B.; Feger, C.; Macknight, W. J.; Schneider, N. S. *Polymer* 1985, 26, 895.
2. Chen, T. K.; Chui, J. Y.; Shieh, T. S. *Macromolecules* 1997, 30, 5068.
3. Xu, M.; Macknight, W. J.; Chen, C. H. Y.; Thomas, E. L. *Polymer* 1983, 24, 1327.
4. Paul, C. J.; Gopinathan Nair, M. R.; Neclakantan, N. R.; Koshy, P.; Idage, B. B.; Bhelhelear, A. A. *Polymer* 1998, 39, 6861.
5. Bunn, C. W. *Proc R Soc Lond A* 180, 1942.
6. Mandelkern, L.; Quinn, F. A.; Roberts, D. E. *J Am Chem Soc* 1956, 78, 926.
7. Faller, R.; Muller-Plathe, F.; Doxastakis, M.; Theodorou, D. *Macromolecules* 2001, 34, 1436.
8. Anandakumaran, K.; Herman, W.; Woodward, A. E. *Macromolecules* 1983, 16, 563.
9. Ravindran, T.; Nayar, M. R. G.; Frans, J. D. *Makromol Chem Rapid Commun* 1986, 7, 159.
10. Quiram, D. J.; Register, R. A. Marchand, G. R. *Macromolecules* 1997, 30, 4551.
11. Wright, K. J. Lesser, A. J. *Macromolecules* 2001, 34, 3626.
12. Shiomi, T.; Takeshita, H.; Kawaguchi, H.; Nagai, M.; Takenaka, K.; Miya, M. *Macromolecules* 2002, 35, 8056.
13. Kim, B. K.; Lee, S. Y.; Baek, S. H. *Polymer* 1998, 39, 2803.
14. Lee, H. Y.; Jeong, H. M.; Lee, J. S.; Kim, B. K. *Polym J* 2000, 32, 23.
15. Leeper, H. M.; Schlesinger, W. *J Polym Sci* 1953, 11, 307.
16. Ravindran, T.; Nayar, M. R. G.; Francis, D. J. *J Appl Polym Sci* 1988, 35, 1227.
17. Brunette, C. M.; Hsu, S. L.; Macknight, W. J.; Schneider, N. S. *Polym Eng Sci* 1981, 21, 163.
18. Cornell, S. W.; Koenig, J. L. *Macromolecules* 1969, 2, 540.
19. Paik Sung, C. S.; Schneider, N. S. *Macromolecules* 1975, 8, 68.
20. Boochathum, P.; Shinizu, M. *Polymer* 1993, 34, 2564.
21. Hopff, H.; Susich G. V. *Rubber Chem Technol* 1931, 4, 75.
22. Edward, G. L.; David, C. W. *J Polym Sci, Part A2* 1969, 7, 1639.
23. Yan, R. F. DE 3227757, 1984.
24. Kim, B. K.; Lee, S. Y.; Xu, M. *Polymer* 1996, 37, 5781.
25. Ozawa, T. *Polymer* 1971, 12, 150.
26. Gopakumar, T. G.; Ghadage, R. S.; Ponrathnam, S.; Rajan, C. R.; Fradet, A. *Polymer* 1997, 38, 2209.
27. Gupta, A. K.; Purwar, S. N. *J Appl Polym Sci* 1984, 29, 1595.